2Pb4-5

Proceedings of Symposium on Ultrasonic Electronics, Vol. 32 (2011) pp. 241-242
8-10 November, 2011

# Properties of Miniature Ultrasonic Motor using $(Sr,Ca)_2NaNb_5O_{15}$ Piezoelectric Ceramics Under High-Input Power

$(Sr,Ca)_2NaNb_5O_{15}$ 圧電体セラミックスを用いた型超音波モータの高入力電力下での特性

Yutaka Doshida[1†], Hiroyuki Shimizu[1], Taisei Irieda[1], Hideki Tamura[2]
([1]Taiyo Yuden Co., Ltd., [2]Tohoku Institute of Technology)
土信田豊 [1‡], 清水寛之 [1], 水野洋一 [1], 田村英樹 [2] ([1] 太陽誘電㈱, [2] 東北工大)

## 1. Introduction

There is a great demand for microactuators to miniaturize mechanical components and add high functionality in mobile equipment. Piezoelectric actuators using $Pb(Zr,Ti)O_3$ (PZT) ceramics have been partly put to practical use and many studies on ultrasonic micromotors have been carried out. As pioneering work, we succeeded in realizing a double-mode miniature cantilever-type ultrasonic motor using lead-free multilayer piezoelectric ceramics (MLPC) of $(Sr,Ca)_2NaNb_5O_{15}$ (SCNN) and the motor showed to be able to rotate by a lithium-ion cell used in the mobile equipment without an amplifier circuit.[1, 2]

However, these miniature piezoelectric devices easily experience a large strain when subjected to a practical value of displacement. Under such a large strain, these miniature piezoelectric devices easily produce a notable degree of nonlinearity as high-power properties. Recently, SCNN ceramics exhibited the jump phenomena with hard-spring effect shown in **Fig. 1** and to posses superior high-power properties than those of PZT ceramics shown in **Fig. 2**.[3]

In this study, we investigated the diriving properties of the motor using SCNN ceramics under high-input power by comparison of their high-power properties.

## 2. Motor design

The picture of the miniature cantilever-type ultrasonic motor using array-type MLPC integrated four pieces of MLPC of SCNN (SCNN-A-MLPC) is shown in **Fig. 3**. The motor can rotate by the first-bending-vibration-mode rotation of the cantilever when oscillated thickness vibration of two pairs of MLPC arranged diagonally in A-MLPC. The driving properties of motor can be designed from the revolution-speed-oriented motor to the torque-oriented one by selecting of vamplate radius of cantilever ($r_v$) shown in **Fig. 4**.[4] In this study, we selected the torque-oriented type motor with $r_v$ = 2.5 mm, because it is easy to evaluate the driving properties of the motor under high-input power.

## 3. Motor characterization

The driving properties of the motor were evaluated under the input power density of 10-25 W/cm$^3$ on SCNN-A-MLPC. The temperature of SCNN-A-MLPC was almost the same of the atmosphere temperature during the evaluation.

**Figure 5** shows the revolution speed as a function of the frequency for the motor. The revolution speed increased up to a peak at the resonance frequency, after which it showed a steep decline. The tendency corresponded to the jump phenomena shown in **Fig. 1**.

**Figure 6** shows the driving properties of the motor. The revolution speed, torque, and efficiency were 180 rpm, 0.14 mN m, and 2.5%, respectively. Furthermore, the output power density on SCNN-A-MLPC was larger than that of ring-type ultrasonic motor with PZT ceramics in practical use. It is caused that the degradation of the quality factor of SCNN ceramics was limited than PZT ceramics. It is expected that the motor using SCNN ceramics have a higher potential than that of PZT ceramics.

## References

1. Y. Doshida, S. Kishimoto, K. Ishii, H. Kishi, H. Tamura, Y. Tomikawa, and S. Hirose: Jpn. J. Appl. Phys. **46** (2007) 4921.
2. Y. Doshida, S. Kishimoto, T. Irieda, H. Tamura, Y. Tomikawa, and S. Hirose: Jpn. J. Appl. Phys. **47** (2008) 4242.
3. Y. Doshida, H. Shimizu, Y. Mizuno, K. Itoh, S. Hirose, and H. Tamura: to be published in Jpn. J. Appl. Phys.
4. Y. Doshida, H. Shimizu, T. Irieda, H. Tamura, Y. Tomikawa, and S. Hirose: Jpn. J. Appl. Phys. **49** (2010) 07HE25.

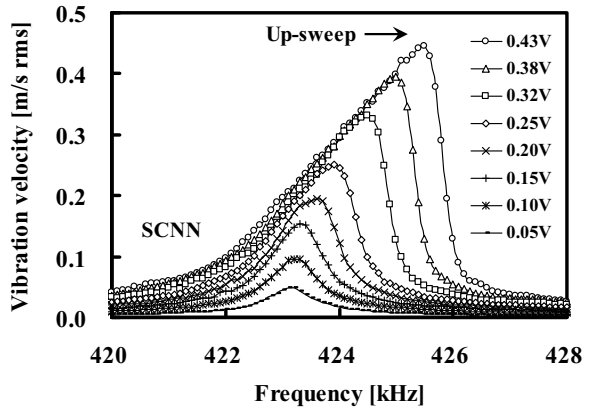


Fig. 1. Jump phenomena under constant-voltage driving for SCNN disk.

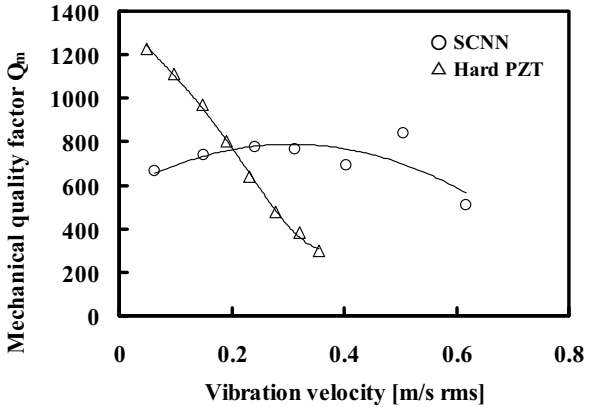


Fig. 2. Vibration velocity dependence of quality factor for SCNN and hard PZT disks.

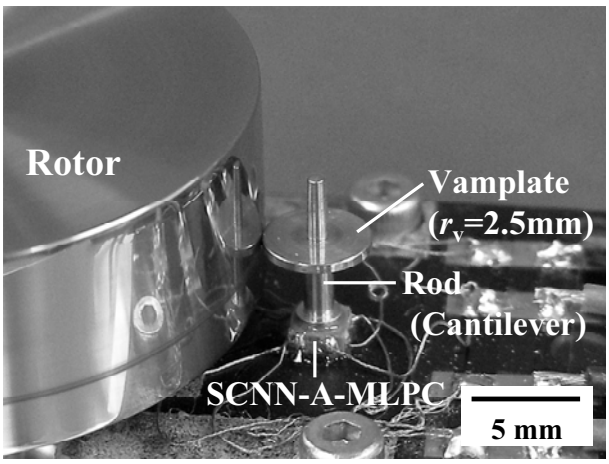


Fig. 3. Picture of cantilever-type ultrasonic motor for SCNN-A-MLPC.

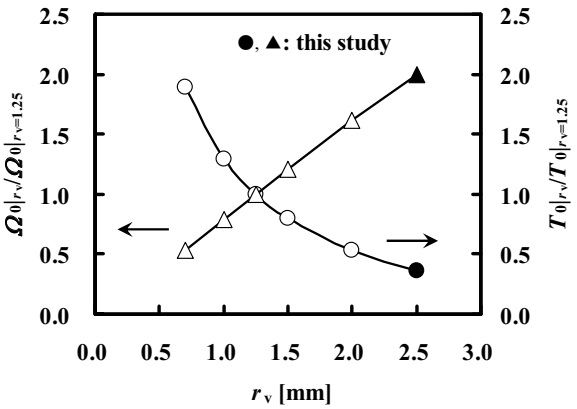


Fig. 4. Simulated result of vamplate radius dependence of maximum revolution speed ($\Omega_0$) and torque ($T_0$).

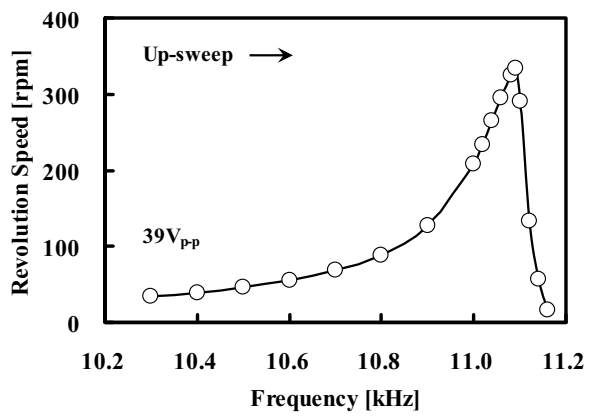


Fig. 5. Revolution speed vs. frequency characteristics for SCNN motor.

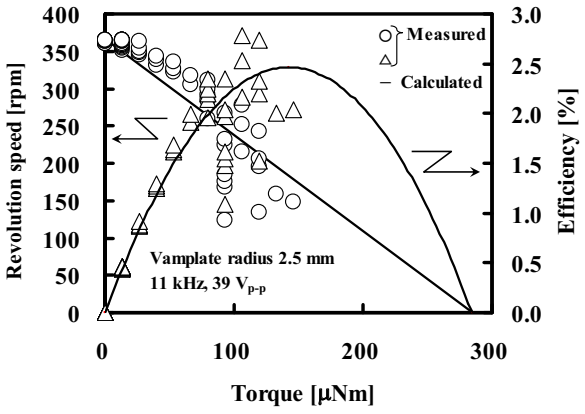


Fig. 6. Relationship among revolution speed, efficiency, and torque for SCNN motor.